Cold Spray Forming of Inconel 718

W. Wong, E. Irissou, P. Vo, M. Sone, F. Bernier, J.-G. Legoux, H. Fukanuma, and S. Yue

(Submitted June 28, 2012; in revised form September 14, 2012)

Inconel 718 was cold spray formed to a 6-mm thickness on an 8-cm diameter aluminum alloy tube using Sulzer Amdry 1718 powder and the Plasma Giken PCS-1000 cold spray system. The effects of spray particle velocity and post-spray heat treatment were studied. Post-spray annealing was performed from 950 to 1250 °C for 1-2 h. The resulting microstructures as well as the corresponding mechanical properties were characterized. As-sprayed coatings exhibited very low ductility. The tensile strength and ductility of the heat-treated coatings were improved to varying levels depending on the heat-treatment and spray conditions. For coatings sprayed at higher particle velocity and heat treated at 1250 °C for 1 h, an elongation of 24% was obtained. SEM micrographs showed a higher fraction of interparticle metallurgical bonds due to some sintering effect. Corresponding fracture surfaces also revealed a higher fraction of dimple features, typically associated with ductile fracture, in the annealed coatings. The results demonstrate that cold spray forming of Inconel 718 is feasible, and with appropriate heat treatment, metallurgical bonding can be increased. The ductility of the spray-formed samples was comparable to that of the bulk material.

1. Introduction

Cold gas dynamic spray (cold spray) is a coating technique that uses high-pressure compressed gas to propel micron-sized solid particles onto a substrate under atmospheric conditions (Ref 1, 2). Upon impact, the powder particles plastically deform, and, if they reached a critical velocity, adhere to form a coating (Ref 3-5). With cold spray, there is tremendous potential to manufacture thick coatings because of its ability to produce dense coatings with minimal heat input (Ref 6, 7). Thus, cold spray makes it possible to spray form or repair components (Ref 8). For

W. Wong, E. Irissou, F. Bernier, and **J.-G. Legoux**, National Research Council Canada, Boucherville, QC, Canada; **P. Vo**, National Research Council Canada, Boucherville, QC, Canada and, Department of Mining and Materials Engineering, McGill University, Montreal, QC, Canada; **M. Sone** and **H. Fukanuma**, Plasma Giken Co., LTD., Tokyo, Japan; and **S. Yue**, Department of Mining and Materials Engineering, McGill University, Montreal, QC, Canada. Contact e-mail: eric.irissou@cnrc-nrc.gc.ca.

the aerospace industry, the cost for materials and machining may represent up to 90% of the manufacturing cost. Cold spray is expected to reduce these costs by up to 40%, which represents significant cost savings for the industry. However, high critical velocity, residual stresses, and technical issues such as nozzle clogging have limited the number of aerospace materials that have been cold spray formed (Ref 5, 9-11). For example, cold spray forming of nickel-based superalloys (i.e., Inconel 718) has been a challenging task to accomplish mainly because of nozzle clogging. This problem has been recently solved in commercial cold spray equipment by using a non-clogging nozzle material combined with a nozzle water cooling system. Karthikeyan and Kay (Ref 12) first demonstrated that it was possible to cold spray deposit Inconel 718; however, process conditions and characterization data have not been reported. Marrocco et al. (Ref 13) produced relatively dense coatings (~95-97%) from fine and coarse 718 powders that displayed hardening near the coating-substrate interface (~150 $HV_{0.1}$ increase relative to the bulk hardness) and relatively low bond strength values (13 MPa) in the as-sprayed condition. Owing to the limited number of studies on cold-sprayed Inconel 718, many mechanical properties, however, remain unavailable.

The mechanical properties of cold-sprayed coatings are significantly influenced by the coating microstructure and in particular, particle bonding. The bonding mechanism has been investigated in many studies (Ref 2, 14-19) with the consensus view being that bonding occurs as a combination of metallurgical bonding due to adiabatic shear instability (ASI) and mechanical bonding due to mechanical interlocking or mixing. Assadi et al. (Ref 14) showed that ASIs are developed by the high strain deformation obtained near the particle-substrate interface, which disrupts the oxide layer and provides an avenue for metallurgical bonding between surfaces. The overall quality of bonding is dependent on material and

process conditions, such as material strength, particle velocity, process temperature, etc. (Ref 10, 14, 19). The bond strength has been modelled as a function of metallurgical and mechanical bondings (Ref 15) with the former capable of being evaluated through a number of methods (Ref 20) including jetting of interfacial material (Ref 14), particle boundaries similar in appearance to grain boundaries after etching (Ref 21, 22), and/or elemental diffusion across particle boundaries (Ref 15, 20). Gartner et al. (Ref 21) showed that increasing the area of well-bonded particles by annealing copper coatings at different conditions correlated to ductility improvements and an associated change in fracture surface. The change in strength was process dependent, however, with the strength of coatings sprayed with propelling gases of nitrogen and helium showing an increase and decrease, respectively, after annealing. The marked effect of annealing on coating tensile properties has also been shown for different materials (Ref 23-25).

In this study, Inconel 718 powder was cold sprayed using Plasma Giken PCS-1000 equipment to produce 6-mm-thick coatings on 8-cm-diameter aluminum tubes using both helium and nitrogen as the propelling gasses. The spray-formed parts were sectioned to produce several samples for material characterization through scanning electron microscope (SEM) and for mechanical tensile testing. The effect of post-sprayed heat treatment was also investigated.

2. Experimental

2.1 Feedstock Powder

Commercially available Inconel 718 powder manufactured by Sulzer Metco (Amdry 1718, Sulzer Metco (US) Inc., Troy, MI, USA) was used. The powder size distribution was measured using a laser diffraction particle size analyzer (Model LS 320, Beckman Coulter, Miami, FL, USA). Figure 1(a) shows the particle size distribution of the Inconel 718 feedstock powder. The mean particle size was 37 μm. Figure 1(b) shows the spherical morphology of the Inconel 718 feedstock powder, while Fig. 1(c) shows an as-polished cross section. The latter micrograph indicates that the particles were nonporous.

2.2 Cold Spray Parameters

Coatings were produced with the PCS-1000 (Plasma Giken Co., Tokyo, Japan) cold spray equipment. The spray parameters using nitrogen gas include the following: propelling gas pressure and temperature of 5 MPa and 1000 °C, respectively; a nozzle standoff distance of 25 mm; a substrate holder rotation speed of 600 rpm; and a gun traverse speed of 10 mm/s. The coating produced was approximately 6 mm thick. Similar spray parameters were used with helium as the propelling gas; the only exception was that an inlet gas pressure of 2 MPa was used instead of 5 MPa. The Inconel 718 powder was cold sprayed onto 8-cm diameter aluminum tubes.

Particle velocities were measured from the centre jet while the cold spray equipment was in free jet with the
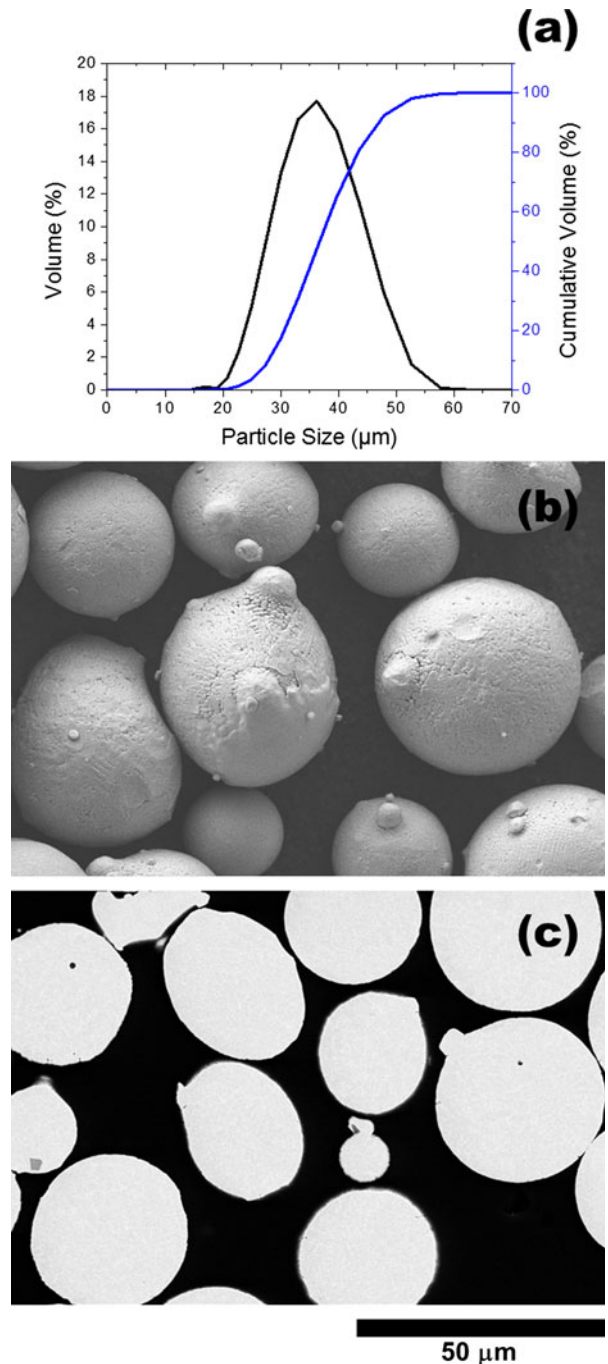

Fig. 1 (a) Feedstock powder size distribution, (b) FEG-SEM micrograph depicting the morphology of the spherical Inconel 718 powder, and (c) as-polished powder cross sections

same cold spray conditions used to produce the coatings using cold spray meter equipment (ColdSprayMeter, Tecnar Automation Inc., St. Bruno, QC, Canada) (Ref 26).

2.3 Sample Extraction and Heat Treatment

The as-sprayed Inconel 718 coatings were sectioned through wire-EDM to extract tensile test samples (perpendicular
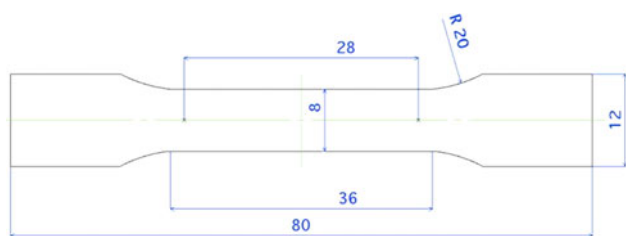
Fig. 2 Dimensions of the tensile test specimens extracted via wire-EDM (all measurements are in mm)

to the plane of spray direction). The dimensions of each tensile specimen are depicted in Fig. 2. Four tensile specimens were kept as-sprayed, while the others were post-heat treated in a furnace under a 90% argon/10% hydrogen atmosphere at 950 °C/2 h, 1010 °C/2 h, 1060 °C/2 h, and 1250 °C/1 h (three samples for each heat treatment). The heat treatments were based on typical batch annealing and HIPing conditions (e.g., 955-1065 °C for 1-3 h (Ref 27) and 1200 °C for 3 h (Ref 28), respectively.

The heat-treatment procedure is outlined below. The samples were placed onto a rectangular metallic stage/holder which was pretreated with boron nitride to prevent the samples from adhering onto the stage/holder. Next, the stage/holder was inserted into a glass tube which has two openings: one end with an opening diameter of 101.6 mm (from which the stage/holder was inserted), and the other end with a small pinhole opening with a diameter of 3.5 mm (for purging air from the glass tube). A specialized cover with a thermocouple and a plastic tube for argon gas flow injection attached to it were then placed and tightened onto the larger glass tube opening. Then, argon gas at 6 standard cubic feet hour (SCFH) was released into the plastic tube for at least 20 min to purge the air from the glass tube and to completely surround the samples in an argon atmosphere (continuous argon gas flow). An air furnace with an opening of the same dimensions as the glass tube was set to 700 °C. When this temperature was reached, the glass tube was partially inserted inside the air furnace and was left there while 10% hydrogen gas was injected into the argon gas flow. When the gas mixture was completed, the tube was fully inserted inside the air furnace where the temperature rose at a constant rate of 10 °C per minute until the desired heat-treatment temperature was reached for each set of coating heat treatments. After the heat treatment was completed, the hydrogen gas was turned off, and the glass tube was partially removed from the air furnace to allow the remaining hydrogen gas to burn. Meanwhile, the tube was left to cool down to room temperature. This was performed while maintaining the continuous argon gas flow atmosphere inside the glass tube until the glass tube reached room temperature, after which the heat-treated samples were removed.

2.4 Metallographic Preparation and Examination

Using standard metallographic preparation procedures, the as-sprayed and heat-treated samples were sectioned with a coolant-assisted diamond wheel, cold vacuum-mounted in an epoxy resin, then ground, and polished. Microstructural observations were performed using a JEOL 840 (JEOL, Tokyo, Japan) scanning electron microscope (SEM) and a Hitachi S-4700 (Hitachi High Technologies America, Inc., Pleasanton, CA, USA) field emission gun scanning electron microscope (FEG-SEM). Powder morphology and coating fracture surfaces were analyzed using FEG-SEM in secondary electron imaging (SEI) mode, while the as-polished coating cross sections were analyzed in backscattered electron imaging (BSI) mode. SEM-BSI mode was also used to conduct coating porosity measurements. These were assessed on the as-polished samples by means of image analysis software (Clemex Vision PE, Clemex Technologies Inc., Longueuil, QC, Canada). A minimum of ten random images were taken, and porosity was evaluated for each image.

2.5 Tensile Testing

Tensile tests were performed in accordance with the ASTM E8/E8M-09 standard (Ref 29) using an Instron 5582 universal testing machine (Instron Canada Inc., Burlington, ON, Canada) with a dynamic load up to 100 kN at a constant speed of 0.05 mm/s. All tests used an extensometer over a gage length of 25 mm.

3. Results and Discussion

3.1 Particle Velocity Measurements

The average particle velocity measured in the centre of the free jet was found to be 787 and 741 m/s for the nitrogen and helium spray conditions, respectively. The particle velocity for nitrogen-sprayed coatings was faster than those sprayed with helium, possibly because (i) although the inlet gas temperature was set to 1000 °C in both cases, the inlet gas pressure was significantly lower when using helium as the propelling gas (2 versus 5 MPa); and (ii) the cold spray gun nozzle was the same for the two gases, while the nozzle design was possibly more optimized for nitrogen fluid dynamics. Thus, although the impacting particle velocity is usually higher with constant conditions when using helium as the propelling gas (Ref 30), in this specific situation, the particle velocity was faster when using nitrogen as the propelling gas.

3.2 As-Sprayed and Heat-Treated Cold-Sprayed Inconel 718 Coating Characterizations

The porosity and the standard error of the as-sprayed and heat-treated coatings are presented in Table 1 for the two particle velocities, V_p. The as-cold-sprayed and heat-treated coatings using the higher particle velocity (787 m/s) condition were found to be slightly denser (1.9-2.7% porosity) than those produced using the lower velocity (741 m/s) condition (3.3-3.8% porosity).

Cross sections of the as-sprayed and heat-treated cold-sprayed Inconel 718 coatings formed from the two particle velocities are shown in Fig. 3 and 4, respectively.

Table 1 Coating porosity of as-sprayed and heat-treated samples

	Porosity %	
Coating treatment	$V_p = 787$ m/s	$V_p = 741$ m/s
As-sprayed	2.7 ± 0.4	3.4 ± 0.4
Heat treated at 950 °C/2 h	2.4 ± 0.2	3.3 ± 0.5
Heat treated at 1010 °C/2 h	1.9 ± 0.2	3.7 ± 0.3
Heat treated at 1060 °C/2 h	2.8 ± 0.2	3.7 ± 0.4
Heat treated at 1250 °C/1 h	2.0 ± 0.6	3.8 ± 0.3

Although the difference in porosity values obtained from the two particle velocity conditions was small, a noticeable difference could easily be seen from visual inspection of Fig. 3 and 4. Thus, the relatively small (~5%) difference in particle velocity corresponded to a small, but noticeable difference in porosity. For coatings sprayed with a constant particle velocity (either 787 or 741 m/s), the coating porosity level remained relatively similar regardless of the coating treatment (as-sprayed or heat treated). In all cases (Fig. 3, 4), the pore distributions were relatively homogeneous throughout the coating cross sections. However, closer observations have revealed that, for the coating sprayed with higher particle velocity and subsequently heat treated at 1250 °C for 1 h (Fig. 3e), its microstructure showed a distinct feature: the interparticle boundaries were almost invisible compared with all other coatings investigated. This may be due to some sintering effect at this high temperature combined with the initial cold spray conditions.

At higher particle velocity, greater particle plastic deformation is expected to occur with an increased fraction of ASI occurrences between interparticle boundaries (Ref 5, 9, 14, 31, 32). Thus, the as-sprayed coatings using the higher particle velocity were expected to have a lower coating porosity level and consequently, more metallurgical bonding, as also evidenced from the quantitative analyses through image analysis in Table 1. The heat-treatment temperatures were considered sufficient to promote further bonding as sintering of material is generally performed at ~2/3 of the absolute melting temperature in a conventional pressing and sintering operation (Ref 33). For Inconel 718, which has a melting temperature range of 1260-1335 °C, this is equivalent to a temperature range of 750-800 °C. Following heat treatment at a high temperature (1250 °C for 1 h), sintering occurred. During the initial stage of sintering, some metallurgical bonding was already present from ASI during the cold spray process. Neck growth took place when moving from the initial to the intermediate stage, increasing the metallurgically bonded area. Finally, pore spheroidization occurred and in certain cases, these pores may have been replaced by metallurgically bonded interparticle boundaries (Ref 34). Owing to the initially lower coating porosity level in the as-sprayed coatings produced using higher particle velocity (Fig. 3a) as opposed to the lower particle velocity (Fig. 4a), fewer spheroidized pores from the final stage of sintering would be expected for the former. This was confirmed from visual inspection of
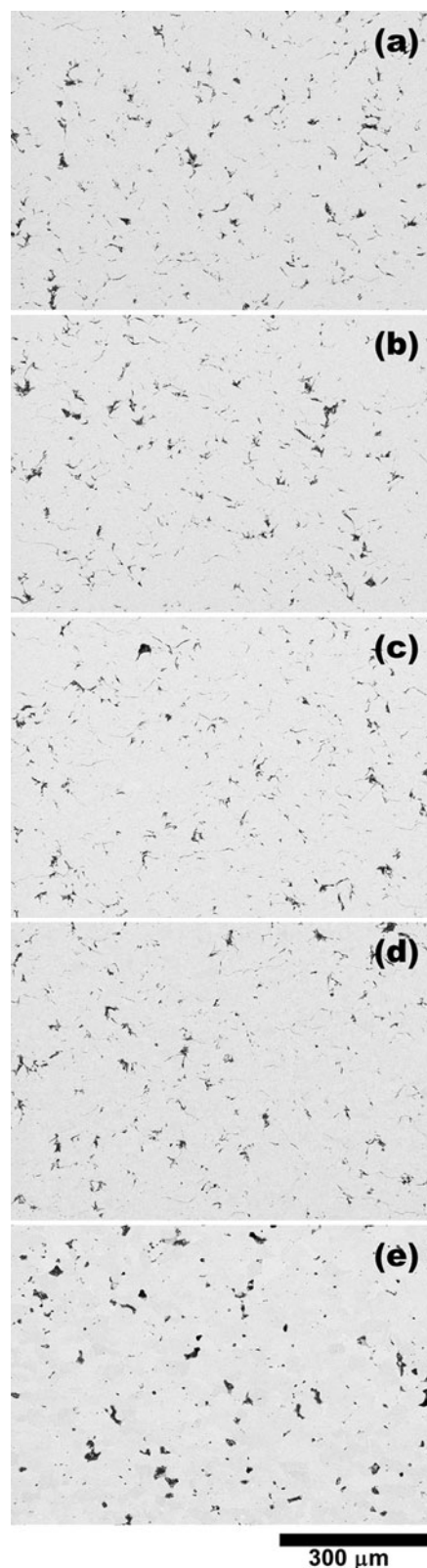

Fig. 3 Cross sections of cold-sprayed Inconel 718 coatings produced with an average particle velocity of 787 m/s: (a) as-sprayed, (b) heat treated at 950 °C/2 h, (c) heat treated at 1010 °C/2 h, (d) heat treated at 1060 °C/2 h, and (e) heat treated at 1250 °C/1 h
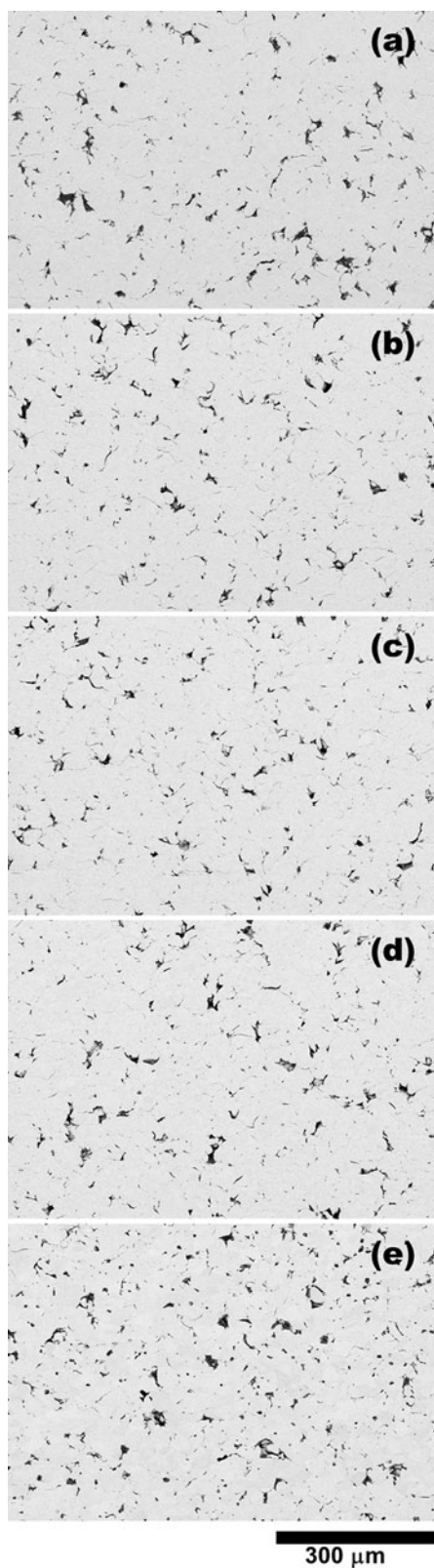
Fig. 4 Cross sections of cold-sprayed Inconel 718 coatings produced with an average particle velocity of 741 m/s: (a) as-sprayed, (b) heat treated at 950 °C/2 h, (c) heat treated at 1010 °C/2 h, (d) heat treated at 1060 °C/2 h, and (e) heat treated at 1250 °C/1 h

Fig. 3(e) and 4(e) at higher magnifications, shown in Fig. 5 and 6, respectively. The red arrows indicate the spheroidized pores after sintering at a high temperature. Thus, this could explain the dissipation of the interparticle boundaries seen in Fig. 3(e) and not in Fig. 4(e).

3.3 Tensile Strength and Ductility

Tensile tests were performed for all coatings presented in Fig. 3 and 4. Examples of the resulting engineering stress versus engineering strain curves are shown in Fig. 7 and 8, respectively. As-sprayed coatings produced at particle velocities of 741 and 787 m/s both exhibited very low ductility (0.18 and 0.23% strain at fracture, respectively), although the latter displayed a higher tensile strength (204 and 277 MPa, respectively).

From Fig. 7 and 8, one can see that regardless of the particle velocity used to produce the Inconel 718 coatings, as the heat-treatment temperature increased, the coating became more ductile (increasing strain). This may be explained by the better interparticle (metallurgical) bonding which resulted from the sintering at the high temperatures.

As expected, the Inconel 718 coating that was as-cold sprayed using the higher particle velocity (787 m/s) and subsequently subjected to a heat treatment at 1250 °C for 1 h revealed the highest ductility by far, with an average strain value of 24.7% from three repeats. This ductility has exceeded specific bulk Inconel 718 sheets that have been solution heat treated and aged (24.7 versus 12% (Ref 35)). On the other hand, the Inconel 718 coating sprayed at the lower particle velocity that was subjected to the same heat treatment only showed an average strain value of 2.2%.

In addition, when comparing Fig. 7 and 8, for the coatings sprayed at the higher particle velocity, increasing heat-treatment temperatures not only increased the fracture strain, but also increased the stress. However, this was not observed for the coatings sprayed at the lower particle velocity, in which increasing heat-treatment temperatures increased the strain but decreased the stress. A tensile strength of 764 MPa was obtained after heat treatment at 1250 °C for 1 h with the coating sprayed at the higher particle velocity, which is approximately 62% of the bulk strength for sheet manufactured in typical annealing and aging conditions (1240 MPa (Ref 35)). As coatings were only tested in the solution heat-treated condition, the experimental tensile strength results did not reflect the substantial precipitation strengthening that would be produced by aging.

Fracture surfaces from tensile test specimens of the as-sprayed and heat-treated cold-sprayed Inconel 718 coatings formed at the higher and lower particle velocities are shown in Fig. 9 and 10, respectively. For the coating produced at the higher particle velocity, smooth fractures with a relatively low overall area of rough dimples were observed in the as-sprayed condition. The dimpled area was greater in annealed coatings and increased with increasing annealing temperature. An almost completely dimple rupture was obtained in the coating annealed at 1250 °C for 1 h. In comparison, the coatings produced at
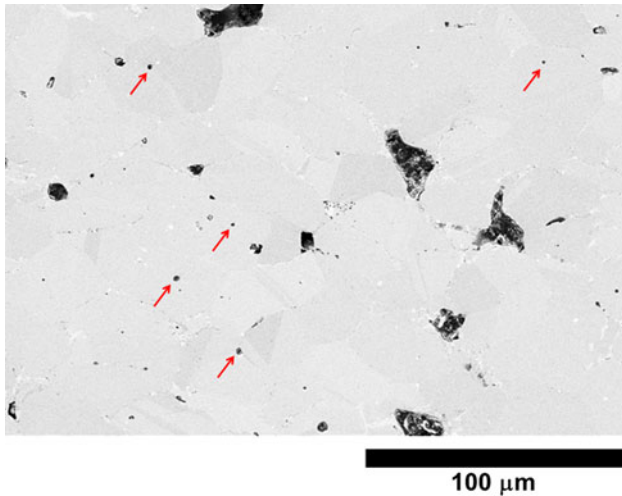
Fig. 5 Cross section of cold-sprayed Inconel 718 coatings produced with a particle velocity of 787 m/s and heat treated at 1250 °C for 1 h
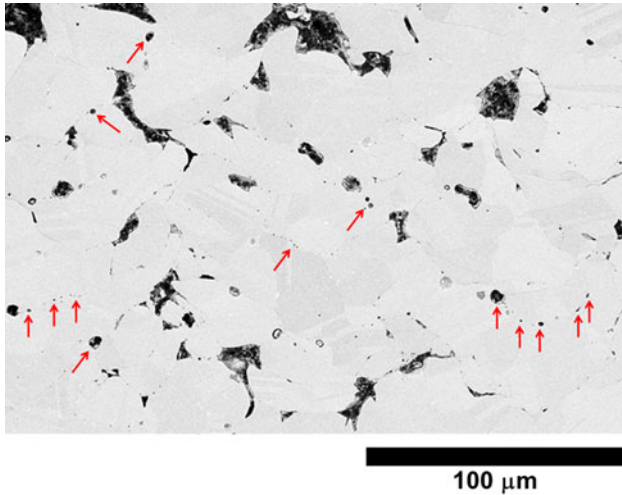

Fig. 6 Cross section of cold-sprayed Inconel 718 coatings produced with a particle velocity of 741 m/s and heat treated at 1250 °C for 1 h

Fig. 7 Tensile test results for as-cold-sprayed and heat-treated Inconel 718 coatings produced with a particle velocity of 787 m/s

Fig. 8 Tensile test results for as-cold-sprayed and heat-treated Inconel 718 coatings produced with a particle velocity of 741 m/s

the lower particle velocity were relatively similar. However, the degree of dimple rupture was less than the higher particle velocity coatings for the respective annealed conditions, particularly at 1250 °C (Fig. 9e, 10e). Although only qualitatively analyzed, the fracture surfaces correlated well with the mechanical data as dimples are a ductile fracture feature and more dimples were observed when higher ductility was obtained (Ref 21).

The lower ductility obtained for the coatings produced at the lower particle velocity may be related to the porosity, which on average, was ~50% higher relative to the levels obtained for the respective coatings produced at the higher particle velocity. In addition, the amount of plastic deformation (i.e., cold work) before the heat treatment was significant. It is well known that the amount of cold work critically influences the ductility of nickel and
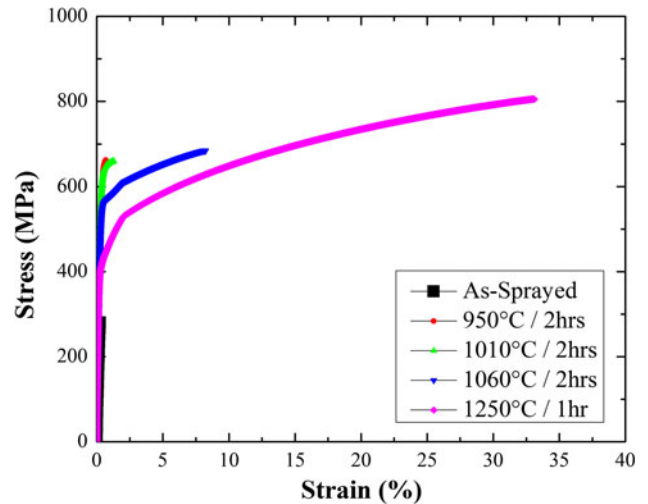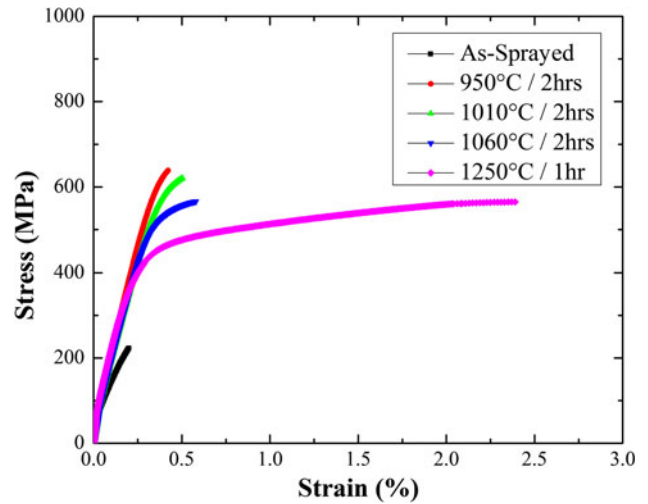
nickel alloys (i.e., Inconel 718) after annealing heat treatments, which are typically performed above 955 °C for approximately an hour (Ref 34). When a low amount of cold work or plastic deformation is present before heat treatment (as is the case with the lower particle velocity condition), full ductility usually cannot be restored by annealing because of excessive grain growth due to critical strain, even if the hardness is recovered to that of the pre-cold worked state (Ref 34). In addition, as the coatings sprayed at the lower particle velocity would have a lower fraction of metallurgically bonded interparticle boundaries after sintering than the coatings sprayed at the higher particle velocity, this would further reduce the likelihood of achieving higher ductility. Thus, a minimum amount of plastic deformation is required to ensure maximum ductility after annealing heat treatments.
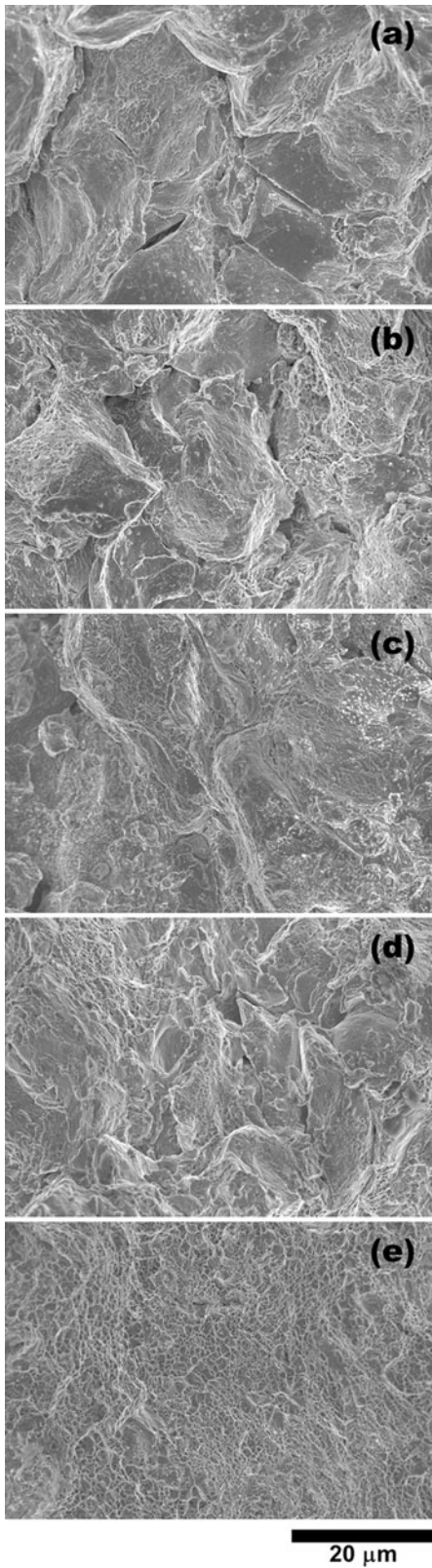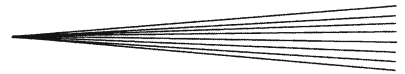
Fig. 9 Fracture surfaces of cold-sprayed Inconel 718 coatings produced with a particle velocity of 787 m/s: (a) as-sprayed, (b) heat treated at 950 °C/2 h, (c) heat treated at 1010 °C/2 h, (d) heat treated at 1060 °C/2 h, and (e) heat treated at 1250 °C/1 h

Fig. 10 Fracture surfaces of cold-sprayed Inconel 718 coatings produced with a particle velocity of 741 m/s: (a) as-sprayed, (b) heat treated at 950 °C/2 h, (c) heat treated at 1010 °C/2 h, (d) heat treated at 1060 °C/2 h, and (e) heat treated at 1250 °C/1 h
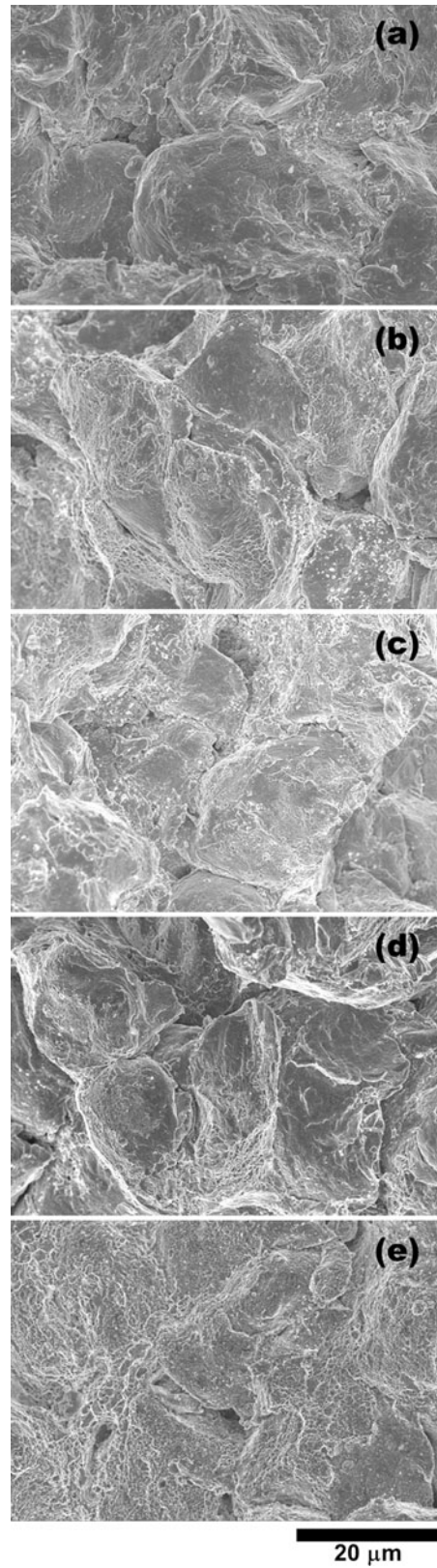
4. Conclusions

The microstructural and mechanical properties of as-sprayed and heat-treated 6-mm-thick cold-sprayed Inconel 718 coatings were investigated. Coating microstructures, porosity, and tensile properties were characterized.

(1) The as-cold-sprayed and heat-treated coatings using the higher particle velocity (787 m/s) condition were found to be slightly denser (1.9-2.7% porosity) than those produced using the lower velocity (741 m/s) condition (3.2-3.8% porosity). In general, coatings sprayed with a constant particle velocity (either 787 or 741 m/s) revealed relatively similar coating porosity levels regardless of the coating treatment (as-sprayed or heat treated).

(2) After heat treatment at 1250 °C for 1 h, the coating sprayed with the higher particle velocity showed a significant amount of interparticle metallurgical bonds, which were not seen in any of the other coatings investigated (i.e., coatings heat treated at the lower temperatures or coatings sprayed at the lower particle velocity). It was hypothesized that this could be due to some sintering effect at this high temperature combined with the initial cold spray conditions which in turn, potentially resulted in high impacting particle velocities and consequently, a large fraction of ASI occurrences.

(3) Enhanced interparticle metallurgical bonds significantly influenced the resulting mechanical properties of the coating such as ductility. From the tensile test results, the highest ductility was found to be at about 24.7% for the Inconel 718 coating sprayed at 787 m/s and subsequently heat treated at 1250 °C for 1 h. The corresponding ultimate tensile stress was about 763.6 MPa, which is approximately 62% of that of the bulk strength.

Acknowledgments

References

1. E. Irissou, J.-G. Legoux, A.N. Ryabinin, B. Jodoin, and C. Moreau, Review on Cold Spray Process and Technology: Part I—Intellectual Property, *J. Therm. Spray. Technol.*, 2008, **17**(4), p 495-516

2. A. Papyrin, V. Kosarev, K.V. Klinkov, A. Alkhimov, and V.M. Fomin, *Cold Spray Technology*, Elsevier Ltd., Oxford, 2006

3. V.K. Champagne, *The Cold Spray Deposition Process: Fundamentals and Applications*, Woodhead Publishing Ltd., Cambridge, 2007

4. R.G. Maev and V. Leshchinsky, *Introduction to Low Pressure Gas Dynamic Spray: Physics & Technology*, WILEY-VCH Verlag GmbH & Co. KGaA, Weinheim, 2008

5. T. Schmidt, F. Gartner, H. Assadi, and H. Kreye, Development of a Generalized Parameter Window for Cold Spray Deposition, *Acta Mater.*, 2006, **54**(3), p 729-742

6. F. Gartner, T. Schmidt, and H. Kreye, Present Status and Future Prospects of Cold Spraying, *Mater. Sci. Forum*, 2007, **534-536**, p 433-436

7. J. Intrater, Cold Spray Technology—Prospects and Applications, *Surf. Eng.*, 2002, **18**(5), p 321-323

8. J. Pattison, S. Celotto, R. Morgan, M. Bray, and W. O'Neill, Cold Gas Dynamic Manufacturing: A Non-Thermal Approach to Freeform Fabrication, *Int. J. Mach. Tool. Manuf.*, 2007, **47**(3-4), p 627-634

9. H. Assadi, T. Schmidt, H. Richter, J.O. Kliemann, K. Binder, F. Gärtner, T. Klassen, and H. Kreye, On Parameter Selection in Cold Spraying, *J. Therm. Spray. Technol.*, 2011, **20**(6), p 1161-1176

10. T. Stoltenhoff, H. Kreye, and H.J. Richter, An Analysis of the Cold Spray Process and Its Coatings, *J. Therm. Spray. Technol.*, 2002, **11**(4), p 542-550

11. F. Gartner, T. Stoltenhoff, T. Schmidt, and H. Kreye, The Cold Spray Process and Its Potential for Industrial Applications, *J. Therm. Spray. Technol.*, 2006, **15**(2), p 223-232

12. J. Karthikeyan and A. Kay, Cold Spray Technology: An Industrial Perspective, *Thermal Spray 2003: Advancing the Science & Applying the Technology*, C. Moreau and B. Marple, Eds., May 5-8, 2003, ASM International, Orlando, FL, 2003, p 117-121

13. T. Marrocco, D. McCartney, P. Shipway, and A.J. Sturgeon, Comparison of the Microstructure of Cold Sprayed and Thermally Sprayed In718 Coatings, *Thermal Spray 2006: Building on 100 Years of Success*, B. Marple, M. Hyland, Y.-C. Lau, R.S. Lima, and J. Voyer, Eds., May 15-18, 2006, ASM International, Seattle, WA, 2006

14. H. Assadi, F. Gartner, T. Stoltenhoff, and H. Kreye, Bonding Mechanism in Cold Gas Spraying, *Acta Mater.*, 2003, **51**(15), p 4379-4394

15. T. Hussain, D.G. McCartney, P.H. Shipway, and D. Zhang, Bonding Mechanisms in Cold Spraying: The Contributions of Metallurgical and Mechanical Components, *J. Therm. Spray Technol.*, 2009, **18**(3), p 364-379

16. A.O. Tokarev, Structure of Aluminum Powder Coatings Prepared by Cold Gasdynamic Spraying, *Met. Sci. Heat Treat.*, 1996, **38**(3), p 136-139

17. D. Goldbaum, R. Chromik, S. Yue, E. Irissou, and J.-G. Legoux, Mechanical Property Mapping of Cold Sprayed Ti Splats and Coatings, *J. Therm. Spray Technol.*, 2011, **20**(3), p 486-496

18. M.P. Dewar, A.G. McDonald, and A.P. Gerlich, Interfacial Heating During Low-Pressure Cold-Gas Dynamic Spraying of Aluminum Coatings, *J. Mater. Sci.*, 2012, **47**(1), p 184-198

19. M. Grujicic, J.R. Saylor, D.E. Beasley, W.S. DeRosset, and D. Helfritch, Computational Analysis of the Interfacial Bonding between Feed-Powder Particles and the Substrate in the Cold-Gas Dynamic-Spray Process, *Appl. Surf. Sci.*, 2003, **219**(3-4), p 211-227

20. T. Price, P. Shipway, D. McCartney, E. Calla, and D. Zhang, A Method for Characterizing the Degree of Inter-Particle Bond Formation in Cold Sprayed Coatings, *J. Therm. Spray Technol.*, 2007, **16**(4), p 566-570

21. F. Gartner, T. Stoltenhoff, J. Voyer, H. Kreye, S. Riekehr, and M. Kocak, Mechanical Properties of Cold-Sprayed and Thermally Sprayed Copper Coatings, *Surf. Coat. Technol.*, 2006, **200**(24), p 6770-6782

22. T. Stoltenhoff, C. Borchers, F. Gartner, and H. Kreye, Microstructures and Key Properties of Cold-Sprayed and Thermally Sprayed Copper Coatings, *Surf. Coat. Technol.*, 2006, **200**(16-17), p 4947-4960

23. S.H. Zahiri, D. Fraser, and M. Jahedi, Recrystallization of Cold Spray-Fabricated Cp Titanium Structures, *J. Therm. Spray Technol.*, 2009, **18**(1), p 16-22

24. A.C. Hall, D.J. Cook, R.A. Neiser, T.J. Roemer, and D.A. Hirschfeld, The Effect of a Simple Annealing Heat Treatment on the Mechanical Properties of Cold-Sprayed Aluminum, *J. Therm. Spray Technol.*, 2006, **15**(2), p 233-238 (236)

25. M.K. Decker, R.A. Neiser, D. Gilmore, and H.D. Tran, Microstructure and Properties of Cold Spray Nickel, *Thermal Spray*
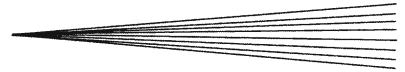
2001: New Surfaces for a New Millenium, C.C. Berndt, K.A. Khor, and E.F. Laguscheider, Eds., May 28-30, 2001, ASM International, Singapore, 2001, p 433-439

26. E. Irissou, J.-G. Legoux, B. Arsenault, and C. Moreau, Investigation of Al-Al$_2$O$_3$ Cold Spray Coating Formation and Properties, *J. Therm. Spray. Technol.*, 2007, **16**(5), p 661-668

27. D.J. Tillack, J.M. Manning, and J.R. Hensley, Heat Treating of Nickel and Nickel Alloys, *ASM Handbook*, Vol 4, S.R. Lampman, T.B. Zorc, J.L. Daqula, and A.W. Ronke, Eds., ASM International, Materials Park, OH, 1991

28. G.A. Rao, M. Srinivas, and D.S. Sarma, Influence of Modified Processing on Structure and Properties of Hot Isostatically Pressed Superalloy Inconel 718, *Mater. Sci. Eng. A*, 2006, **418**, p 282-291

29. "Standard Test Methods for Tension Testing of Metallic Materials," E8/E8M-09, ASTM International, West Conshohocken, PA

30. M. Grujicic, C. Tong, W.S. DeRosset, and D. Helfritch, Flow Analysis and Nozzle-Shape Optimization for the Cold-Gas Dynamic-Spray Process, *Proc. Inst. Mech. Eng. Part B*, 2003, **217**, p 1603-1613

31. W. Wong, E. Irissou, A.N. Ryabinin, J.G. Legoux, and S. Yue, Influence of Helium and Nitrogen Gases on the Properties of Cold Gas Dynamic Sprayed Pure Titanium Coatings, *J. Therm. Spray. Technol.*, 2011, **20**(1-2), p 213-226

32. T. Schmidt, H. Assadi, F. Gartner, H. Richter, T. Stoltenhoff, H. Kreye, and T. Klassen, From Particle Acceleration to Impact and Bonding in Cold Spraying, *J. Therm. Spray. Technol.*, 2009, **18**(5-6), p 794-808

33. E. Klar, Powder Metallurgy, *Metals Handbook Desk Edition*, 2nd ed., J.R. Davis, Ed., ASM International, Materials Park, OH, 1998, p 876-891

34. R.M. German, *Sintering Theory and Practice*, Wiley, New York, 1996

35. R.N. Caron and J.T. Staley, Nickel and Nickel Alloys, *Metals Handbook Desk Edition*, 2nd Ed., J.R. Davis, Ed., ASM International, Materials Park, OH, 1998, p 609-616